Journal of Engineering Science and Technology
Special Issue on Development of Sustainability Systems - II, 145 - 157

NUMERICAL ANALYSIS OF THE HELMET EFFECT ON SOLAR RADIATION AND TEMPERATURE REDUCTION TO AVOID BRAIN STROKE

QUSAY J. ABDUL-GHAFOOR[1], WAJEEH K. HASAN[2], ALI J. ALI[3,*], KARRAR A. HAMMOODI[4], HASAN SHAKIR MAJDI[5]

[1]Mechanical Engineering Department, University of Technology- Iraq, Baghdad, 10066, Iraq
[2]Department of Refrigeration and Air Conditioning Engineering, Al-Rafidain University College, Baghdad, 10001, Iraq
[3]Department of Biomedical Engineering, University of Technology- Iraq, Baghdad, Iraq
[4]Department of Air-Conditioning and Refrigeration Techniques Engineering, University of Warith Al-Anbiyaa, Baghdad Rd, Karbala, 56001, Iraq
[5]Department of Chemical Engineering and Petroleum Industries, Al-Mustaqbal University College, 51001 Hillah, Babylon, Iraq
*Corresponding Author: Ali.j.Ali@uotechnology.edu.iq

Abstract

The research explores the link between solar radiation exposure, brain temperatures, and stroke risk. It highlights the importance of understanding the effects of solar radiation on human health, particularly neurological well-being, due to rising global temperatures. The materials manufactured for the helmet are taken from two layers to improve the thermal insulation of the brain by wearing a helmet. The first layer-representing fiberglass, which is where the value of the conduction coefficient for this layer is 0.363 W/m·℃. The second layer represents the cotton wrapped for the inner layer of the helmet, which has a thermal conductivity value of 0.026 W/m·°C, which is a good heat insulator. Human hair is also an insulator for the heat applied to it, as a layer of hair was made simulating the real state with a thermal conductivity coefficient of 0.37 W/m·°C, and the height of the hair is 1 cm. The human head's back region experiences higher temperatures, reaching 49.31 °C due to heat transfer between the head and brain surface. This affects facial bones and internal organs. Helmets help reduce head temperatures by reflecting and dissipating solar radiation.

Keywords: Biomechanical, Brian layer, Brain stroke, Brain temperature, Sustainable development.

1. Introduction

Solar energy, primarily sunshine, is crucial for life on Earth, but excessive exposure can harm the human body, particularly the brain, due to its delicate thermal equilibrium. Hyperthermia, a condition resulting from increased body temperature, can disrupt this balance, leading to various health issues. Solar radiation indirectly increases the risk of heat-related disorders like heat stroke, which can harm blood vessels and brain tissue. Acute ischemic stroke can be reduced by selective brain hypothermia, allowing simultaneous endovascular blood cooling and mechanical thrombectomy, potentially reducing long-term impairments and fatalities [1].

A slotted disc monopole antenna for the 2.45 GHz ISM radio band was developed and printed on a PET substrate for early brain stroke detection. The antenna has a 480 MHz bandwidth and a frequency range of 2.25 GHz to 2.73 GHz [2]. Temperature affects human organs, especially at the relatively high temperature that occurs during the summer weather in Iraq [3-5]. The study involved 432 participants, with 59% males and a mean age of 65-61%. Results showed that higher pre-EVT temperatures were associated with decreased functional independence and higher mortality, with peak post-EVT temperature being a significant predictor of high modified Rankin Scale scores [6].

The stroke spot and human head phantom were compared using specific absorption rate (SAR) data. The findings demonstrate that Antennas A and D had the lowest SAR values, measuring 1.44 105 W/kg and 1.96 10 W/kg, respectively. Antenna D's superior performance was further supported by its superior 2-D far-field radiation patterns compared to other antennas. The 2-D far-field radiation patterns further supported Antenna D's superior performance compared to the other antennas [7].

In affluent nations, brain strokes were one of the main causes of adult disability and death. Since haemorrhagic stroke is 15%, and ischemic stroke is 85% of all occurrences that need different treatments, the type of stroke was crucial to identify promptly. Microwave tomography can detect changes in the electric permittivity of brain tissues resulting from strokes [8].

The study suggests that using an intra-carotid heat exchange catheter for direct arterial blood cooling could potentially reduce inflammation and apoptosis in stroke patients with significant artery blockage, thereby reducing brain temperature [9]. The study proposes a radio platform for brain care applications inspired by RFID, consisting of spatially dispersed antennas, a cortical implant portion, and a passive wearable component on the scalp. The wireless testing results of the prototyped antenna system indicate that it can remotely power and read out a -18 dBm RFID microsystem at 1.0 m at 915 MHz with a 10 mm implant depth [10].

A panel of specialists has recommended non-pharmacological targeted temperature control for patients with neurogenic fever and bleeding based on current research and pragmatic factors. After doing the necessary workup for infection, targeted temperature control should be started if the patient's temperature climbs over 37.5 ℃. This reduces the need for preventative targeted care and ensures proper infection handling [11, 12]. A heated plastic thermal head form was created to evaluate cycling helmet cooling performance. The form, consisting of a low thermal conductivity 3D-printed head form with a high thermal mass internal layer, was heated to a steady temperature in a wind tunnel [13].

On the cancer tumours in the brain, hyperthermia, a therapeutic method based on temperature sensitivity differences between healthy tissues and malignancies, has emerged as a promising treatment approach for cancer. The elimination of cancer cells occurs when the temperature of the tumour is elevated to 40 - 45 ℃ for a certain amount of time during hyperthermia therapy. The research demonstrated that increasing temperature and concentrating energy deposition in brain tumours can be achieved at therapeutic levels without causing damage to healthy tissue [14].

Functional near-infrared spectroscopy (fNIRS), an optical neuroimaging technique, assesses hemodynamic responses and brain activity by examining factors like frontal sinus volume, scalp-cortex distance, and sulcal architecture [15]. An elevated brain temperature may accelerate tissue metabolism and cause infarction in patients with acute ischemic stroke, potentially causing pyrexia and poor outcomes, as evidenced by multi-voxel magnetic resonance spectroscopic imaging [16].

Magnetic resonance proton spectroscopic imaging (SI) was used to measure regional brain temperatures in human volunteers, revealing high temperatures in abnormal areas and providing accurate data for stroke research [17]. The study used magnetic resonance spectroscopic imaging to measure cerebral temperature in stroke patients, revealing a link between pyrexia and worse outcomes post-stroke. Possible abnormal tissue had a greater temperature of 37.63°C than tissue that was certainly abnormal or had a brain that seemed to be normal [18].

Medical scientists need to investigate brain health consequences from prolonged heat exposure together with cooling therapy assessment. Research conducted by public health scientists ought to evaluate the effect of climate change on stroke development in the human brain while establishing predictive tools for identifying high-risk circumstances.

Through previous research and the mechanism of focusing on the issue of the effect of high temperatures on the human brain, it was necessary to use advanced simulation programs to understand more and reduce the risks of brain injury due to high temperatures that were capable of generating clots that kill a person. In addition to discussing methods to reduce these hazards, this article examines the complex link between solar radiation, brain temperatures, and the risk of stroke. This study is designed to predict the brain and the outer surface temperature of the human head without hair, with hair, and with a helmet. The prediction is performed by numerical simulation using ANSYS software.

2.Materials and Methods

2.1. Materials

After the design process, the model is exported to ANSYS R19.0 software. The simulation process is transferred, and the physical properties of materials used in the layers are entered to know the thermal effect on the brain. The thermal properties of the layers are taken from different resources, as shown in Table 1.

In the process of improving the thermal insulation of the brain by wearing a helmet, the materials manufactured for the helmet are taken from two layers. The first layer represents fibreglass, which is where the value of the conduction coefficient for this layer is 0.363 W/m·℃ [19]. The second layer represents the

cotton wrapped in the inner layer of the helmet, which has a thermal conductivity value of 0.026 W/m·°C [20], which is a good heat insulator. Human hair is also an insulator for the heat applied to it, as a layer of hair was made simulating the real state with a thermal conductivity coefficient of 0.37 W/m·°C, and the height of the hair is 10 mm.

Table 1. Thermal properties of head layers.

Tissues	Density ρ (kg/m^3)	Heat Capacity Cp J/kg·K	Thermal conductivity k (W/m·K)	Metabolic heat generation Q_{met} (W/kg)	Volumetric heat transfer coefficient (W/m^3·K)
Brain / grey matter	1039	3675	0.57	6.833	35000
CSF	1007	4191	0.6	0	0
Fat	916	2524	0.25	0.328	916
Muscles	1041	3546	0.53	0.461	3360
Skin	1100	3437	0.35	1.473	9100
Skull	1990	1300	0.39	0.307	1000

2.2. Computational procedure

2.2.1 Model generation

The simulation process requires designing the geometric model of the head by using SolidWorks software, which is an engineering program that works on designing simulated models using certain formulas. The layers of the brain are taken from previous research [10] and designed as in Fig. 1.

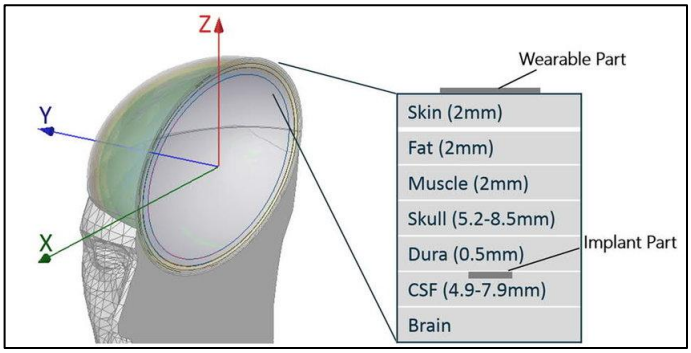

Fig. 1. Head layer [10].

For the process of improving the thermal insulation of the brain, adding hair to the outer layer of the skin and a protective helmet. The domain used in Fig. 2 became the main domain for the simulation process.

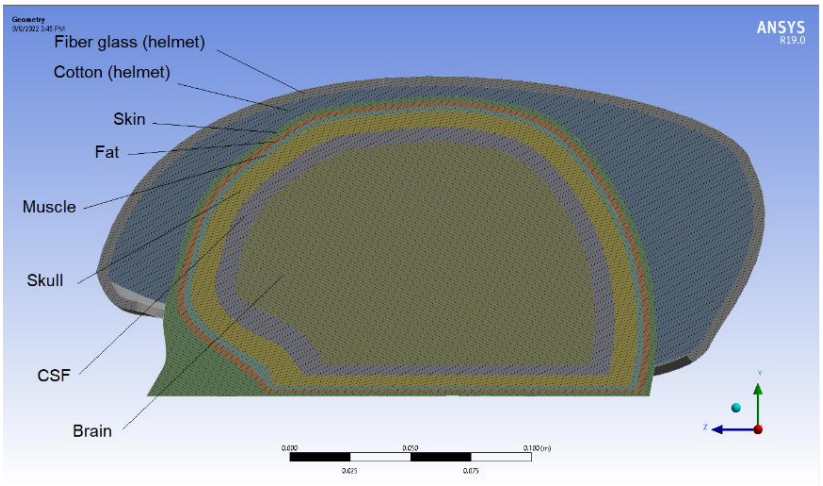

Fig. 2. Simulation domain.

2.2.2 Mesh generation and independency check

The ANSYS R19.0 program uses the meshing process in FEM format to solve algebraic equations. Mesh independence is achieved by increasing the number of elements and narrating the results until they are close to the case before it, ensuring accurate and close results, as in Table 2. Where the steady state reached by the process of the mesh is 3,256,787 elements, in which the temperature of the brainstem in the case of the helmet is 38.86 ℃. The brain mesh scheme is shown in Fig. 3.

Table 2. Mesh independence.

Case	Element No.	Node No.	Max. temperature (ºC)	% of change
1	945,560	638,879	41.546	-
2	1,850,564	1,434,676	38.945	6.260
3	2,674,545	1,954,095	38.861	0.215
4	3,256,787	2,536,687	38.858	0.007

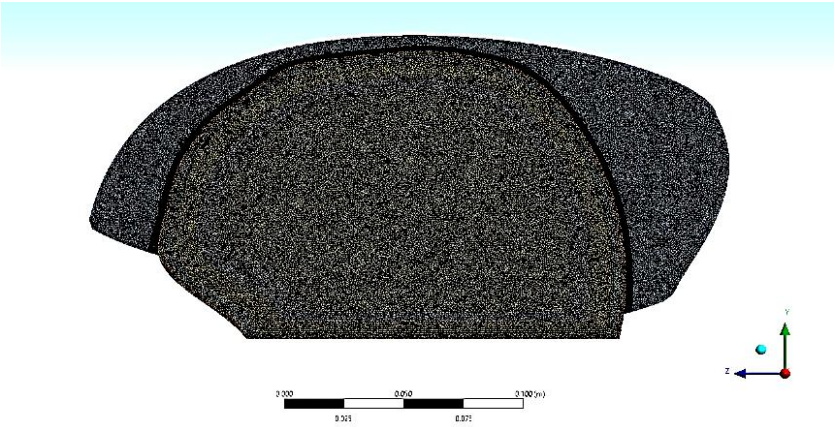

Fig. 3. Mesh domain.

2.2.3 Governing equations

The primary unknowns in a single-field finite element model are the temperatures at different nodes, which can be represented using the following form:

$$\{f(T)\} = [K(T)]\{T\} - q\{Q\} = 0 \quad (1)$$

{f(T)}: describes the temperature distribution at different nodes. Each element of this vector corresponds to the temperature at a specific node.
[K(T)]: a matrix or operator that relates the temperatures at different nodes. It describes how heat is conducted or transferred between the nodes and is dependent on the temperatures at those nodes.
-*q*: represents a source or sink of heat within the system, which affects the temperature distribution.

The steady-state temperature distribution in the system means that the heat input (q{Q}) is balanced by the heat transfer between nodes ([K(T)]{T}).

$$[K(T)] = \left[K^{(k)}\right] + \left[\bar{K}^{(r)}\right] + \left[K^{(h)}\right] \quad (2)$$

and,

$$\{Q\} = \left\{Q^{(o)}\right\} + \left\{Q^{(r)}\right\} + \left\{Q^{(h)}\right\} \quad (3)$$

It appears that you have provided an equation with different terms denoted as $Q^{(o)}$, $Q^{(r)}$, and $Q^{(h)}$. These terms may represent different components or sources of a total quantity represented by Q. To better understand this equation, we can break down the terms:

$Q^{(o)}$: This term likely represents one component or source of the total quantity Q.
$Q^{(r)}$: This term represents another component or source contributing to the total quantity Q.
$Q^{(h)}$: Similarly, this term represents yet another component or source that contributes to the total quantity Q.

The equation provided is essentially summing up these three components $Q^{(o)}$, $Q^{(r)}$ and $Q^{(h)}$ to determine the overall value of Q. This is a common mathematical notation for combining multiple sources or factors to calculate a total or composite value. If it has specific values or equations related to these components $Q^{(o)}$,$Q^{(r)}$ and$Q^{(h)}$, it can provide those details to perform calculations or further analysis based on this equation. For convenience, the material conductivities in the present study are assumed to vary quadratically with temperature, as follows:

$$k_{\alpha\beta} = k^0_{\alpha\beta}(1 + \gamma_1 T + \gamma_2 T^2) \quad (4)$$

where $k^0_{\alpha\beta}$ is the thermal-conductivity coefficient at a preselected reference temperature of $T = 0$, and γ_1 and γ_2 are conductivity coefficients.

The quadratic variation of the material conductivities with temperature, Eq. (4), is adequate for most practical applications. When tabulated data are given for the conductivities as functions of temperature, best quadratic fits can be used in the analysis. In the numerical studies, only isotropic materials are considered, for which $k_{11} = k_{22} = k^0(1 + \gamma_1 T + \gamma_2 T^2)$, and $k_{12} = 0$. In addition, the convection matrix is assumed to be independent of temperature, and the radiation matrix varies

cubically with temperature. The matrices $[K^{(k)}]$ and $[\bar{K}^{(r)}]$ can be expressed in the following forms:

$$[K^{(k)}] = [K^{(0)}] + q_1[K^{(1)}(T)] + q_2[K^{(2)}(T)] \quad (5)$$

and,

$$[\bar{K}^{(r)}] = q_3[K^{(r)}] \quad (6)$$

where $[K^{(0)}]$ is the linear conduction matrix (independent of T); $[K^{(1)}]$ and $[K^{(2)}]$ are normalized nonlinear conduction matrices whose terms are linear and quadratic in the nodal temperatures $\{T\}$; $[K^{(r)}]$ is a normalized radiation matrix, and q_1, q_2, q_3 are normalizing parameters [21].

2.2.4 Boundary conditions

The thermal simulation program was developed, selecting heat flow regions from solar radiation at three different altitude angles, as depicted in Fig. 4.

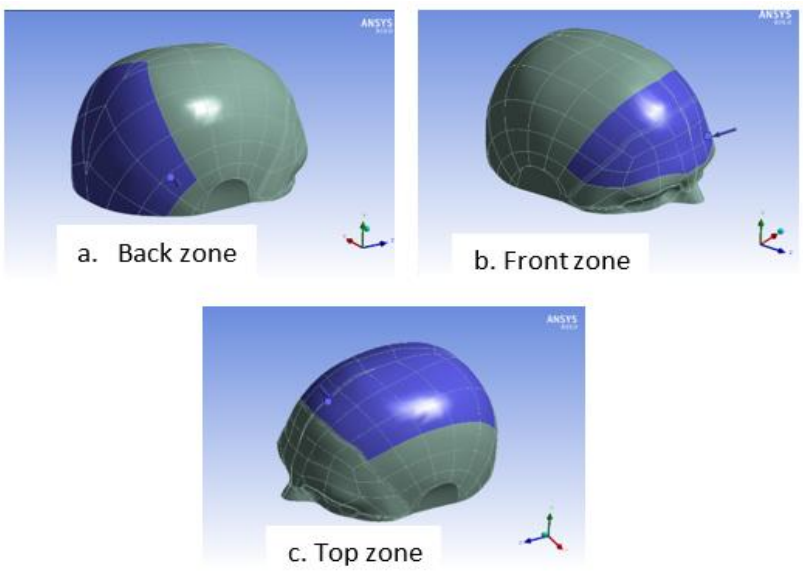

Fig. 4. Heat flux of solar radiation equal to 780 W/m^2 at different altitude angles of radiation: (a) back zone, (b) front zone, and (c) top zone.

The value of the solar radiation falling in Iraq and in the summer at 1 pm represents the largest value of the solar radiation, which is 780 W/m^2. Where the amount of heat transferred by convection and radiation was considered, as a percentage of the amount of heat flowing through the head was taken. As for the second boundary, which represents heat transfer by free convection between the brain and the head, it is known that the value of the internal head temperature in the normal state is 37.5 ^{o}C. It has been proven from the area of heat transfer by free convection in the case of the body in the state of rest. Work was not done in a steady state because in normal conditions in Iraq, a person is walking for an hour or two, and this period delivers the results obtained in a way that is consistent with time.

3. Results and Discussion

The rise in brain temperature in the summer in areas close to the equator has a dangerous effect on the presence of strokes. The results paragraph will be divided according to the different areas of solar radiation and by using materials that reduce the value of heat transmitted to the brain. Previous research has proven that if the brain temperature exceeds 37.5 ºC over a long period, it causes a stroke and other health symptoms, according to a group of samples [12].

3.1. The effect of solar radiation on the brain according to the altitude angle of radiation

The effect of solar radiation on the brain by increasing the temperature varies according to the altitude angle of the projections. Figure 5 shows that the temperature value on the outer surface of the human head rises in the back region more than the rest of the head, where the maximum temperature reached 49.31℃, a high value that significantly affects the vital functions of the human body. The reason for this is that the brain is very close to the posterior region compared to the frontal region, which challenges the facial bones and the many frontal internal organs.

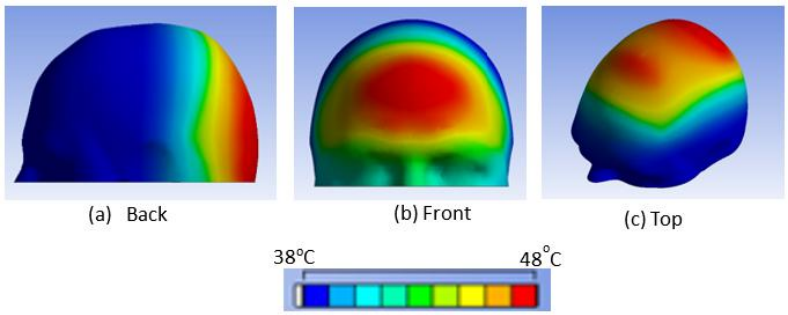

Fig. 5. Temperature contour at different altitude angles on the outer surface of the human head: (a) back zone, (b) front zone, and (c) top zone, without helmet.

As for the temperatures affecting the brain and in the different areas of solar radiation, it is noted in Fig. 6 that the maximum temperature value in the upper region of the brain was 42.052 ℃. High temperatures in the head and brain due to the lack of an insulator between the head and sun and the large area of temperature transfer between the epidermis and brain surface lead to fatal strokes.

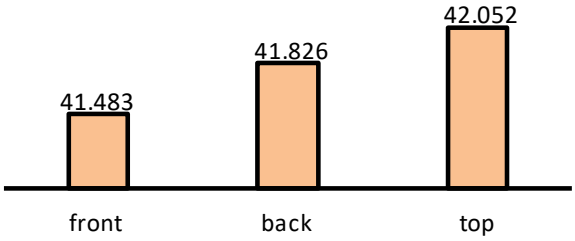

Fig. 6. Maximum temperature in middle line at different locations in brain surface.

3.2. The effect of hair and helmet on brain temperatures

Human head hair lowers the head temperature, affecting brain temperature. Helmets reduce collision damage and head temperatures during high temperatures, helping to protect cyclists and motorcycle drivers from brain damage. Figure 7 shows that the predicted temperature when the helmet is in place decreases up to 39.9 ℃ from around 42.0 ℃ without hair and 41.7 ℃ with hair. The predicted temperatures are on the outer surface of the body, once on the helmet, second on the head and third on the hair. The helmet's high surface area value and the ability of its materials to absorb and convert solar radiation make it a valuable tool to reduce the solar heating of the human head.

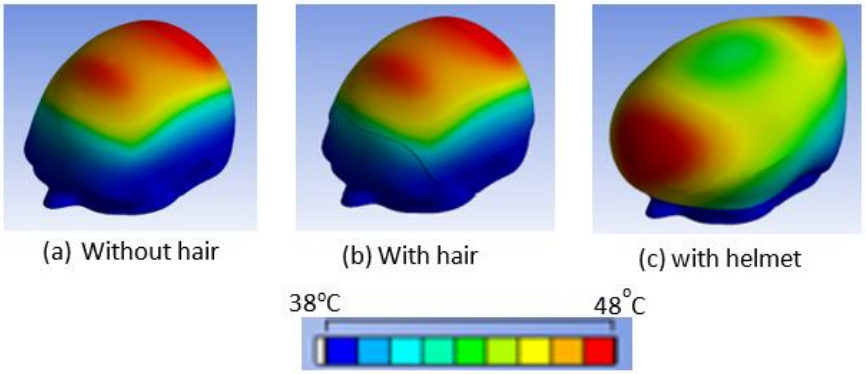

Fig. 7. Temperature contour on the outer surface (a) without hair, (b) with hair, and (c) with helmet.

As for the outer surface of the brain, the effect of the helmet on reducing the heat transmitted by contact between the layers of the brain and thus reducing the brain temperature. The helmet reduced the temperature to 38.86 ℃, which is a safe degree for the brain to protect it from fatal strokes, in contrast to the absence of a helmet whose temperature value has reached 42 ℃, which is a dangerous temperature, as in Fig. 8.

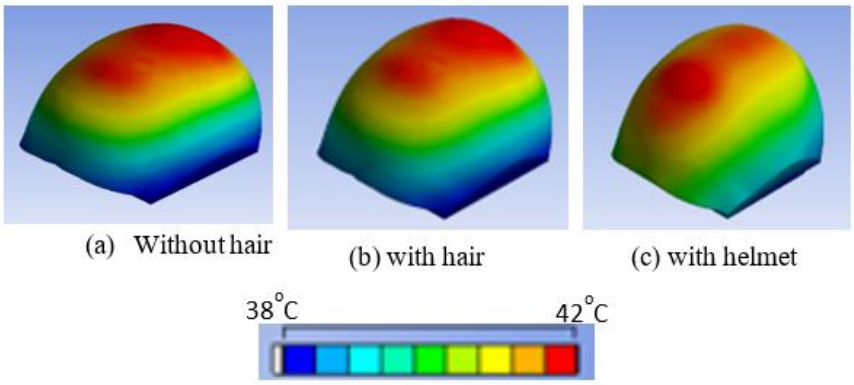

Fig. 8. Temperature contour in brain surface: (a) without hair, (b) with hair, and (c) with a helmet.

Figure 9 displays the predicted maximum temperature on the dead surface. The results in the figure show a comparison between cases of the head without hair, with hair, and when the head is covered with a helmet. A great improvement is observed in isolating the arrival of high temperatures to the brain to ensure that a person does not suffer a stroke in Iraq in the summer. In an average presentation, the helmet reduces the maximum temperature by around 7.3%, 8.0%, and 8.2% on the front, the back, and the top of the head, respectively.

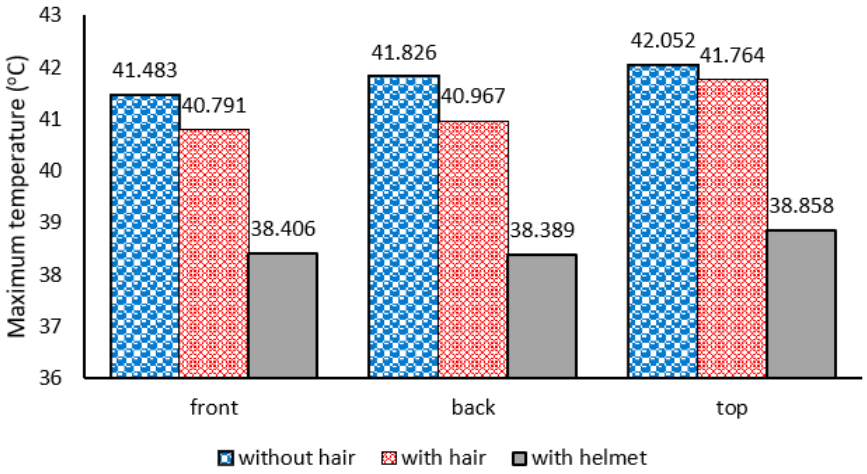

Fig. 9. Maximum temperature of different conditions with different locations on the head.

The prevention of strokes depends on controlling blood pressure through maintaining a healthy diet, exercising moderately, and reducing stress while controlling blood pressure. The installation of cooling infrastructures in urban planning alongside advance helmet systems equipped with temperature sensors alongside heat-resistant building materials helps decrease heat-related dangers.

4. Conclusions

The study explores the link between sun radiation exposure, brain temperatures, and stroke risk, emphasizing the need to understand the effects of solar radiation on human health, particularly neurological well-being, especially as global temperatures rise. The results will be summarized as follows:

- The findings of this work concluded that the temperature in the human head rises in the back region more than the rest of the head, where the maximum temperature reached 49.31 ℃.
- The maximum temperature in the upper region of the brain was 42.05℃, which is a very high value that leads to fatal strokes due to the absence of an obstacle or insulator between the head and the sun.
- The helmet is designed to minimize collision damage and, in high temperatures, to reduce head temperatures. The temperature value when the helmet is in place increases up to 55.9 ℃.

The field needs further investigation regarding improved heat insulation materials and computational simulation frameworks for brain temperature modelling. In addition, sensor data collection approaches for real-world testing. AI-driven risk monitoring systems, along with portable brain cooling devices, enable advanced methods for preventing heat-related emergencies through enhanced response measures.

Nomenclatures

A	Surface area, m²
c_p	Specific heat capacity, J/kg·K
k	Thermal conductivity, W/m·K
M	Mass, kg
P	Pressure, Pa
Q_{met}	Metabolic heat generation, W/kg
q	Heat flux, W/m²
R	Thermal resistance, K/W
T	Temperature, °C
v	Velocity, m/s

Greek Symbols

α	Thermal diffusivity, m^2/s
β	Thermal expansion coefficient, 1/K
δ	Thickness of insulation layer, m
ϵ	Emissivity
ϕ	Solar radiation angle, Degree
γ	Gravitational acceleration, m/s^2
λ	Wavelength of radiation, nm
μ	Dynamic viscosity, Pa.s
ν	Kinematic viscosity, m^2/s
ρ	Density, kg/m^3
σ	Stefan-Boltzmann constant, 5.67×10^{-8} W/m²·K⁴
τ	Transmissivity of material

References

1. Lutz, Y.; Meiner, T.; Krames, L.; Cattaneo, G.; Meckel, S.; Dossel, O.; and Loewe, A. (2021). Selective Brain hypothermia for ischemic MCA-M1 stroke: Influence of cerebral arterial circulation in a 3D brain temperature model. *IEEE Transactions on Biomedical Engineering*, 68(2), 404-415.
2. Rahman, M.A.; Hossain, M.F.; Riheen, M.A.; and Sekhar, P.K. (2020). Early brain stroke detection using flexible monopole antenna. *Progress in Electromagnetics Research C*, 99, 99-110.
3. Gaznayee, H.A.A.; Al-Quraishi, A.M.F.; Mahdi, K.; and Ritsema, C. (2022). A geospatial approach for analysis of drought impacts on vegetation cover and land surface temperature in the Kurdistan Region of Iraq. *Water*, 14(6), 927.
4. Al-Ghezi, M.K.; Ahmed, R.T.; and Chaichan, M.T. (2022). The influence of temperature and irradiance on performance of the photovoltaic panel in the middle of Iraq. *International Journal of Renewable Energy Development*, 11(2), 501-513.

5. Salman, S.A. et al. (2022). Projecting spatiotemporal changes of precipitation and temperature in Iraq for different shared socioeconomic pathways with selected coupled model intercomparison project phase 6. *International Journal of Climatology*, 42(16), 9032-9050.
6. Diprose, W.K. et al. (2020). Impact of body temperature before and after endovascular thrombectomy for large vessel occlusion stroke. *Stroke*, 51(4), 1218-1225.
7. Smida, A. (2020). Simulation and analysis of variable antenna designs for effective stroke detection. *International Journal of Advanced Computer Science and Applications*, 11(12), 238-244.
8. Coli, V.L.; Tournier, P.-H.; Dolean, V.; Kanfoud, I.E.; Pichot, C.; Migliaccio, C.; and Blanc-Feraud, L. (2019). Detection of simulated brain strokes using microwave tomography. *IEEE Journal of Electromagnetics, RF and Microwaves in Medicine and Biology*, 3(4), 254-260.
9. Lutz, Y.; Loewe, A.; Meckel, S.; Dössel, O.; and Cattaneo, G. (2019). Combined local hypothermia and recanalization therapy for acute ischemic stroke: Estimation of brain and systemic temperature using an energetic numerical model. *Journal of Thermal Biology*, 84, 316-322.
10. Ma, S.; Sydanheimo, L.; Ukkonen, L.; and Bjorninen, T. (2018). Split-ring resonator antenna system with cortical implant and head-worn parts for effective far-field implant communications. *IEEE Antennas and Wireless Propagation Letters*, 17(4), 710-713.
11. Andrews, P.J.D.; Verma, V.; Healy, M.; Lavinio, A.; Curtis, C.; Reddy, U.; Andrzejowski, J.; Foulkes, A.; and Canestrini, S. (2018). Targeted temperature management in patients with intracerebral haemorrhage, subarachnoid haemorrhage, or acute ischaemic stroke: Consensus recommendations. *British Journal of Anaesthesia*, 121(4), 768-775.
12. Taccone, F.S.; Donadello, K.; and Mayer, S.A. (2022). Manipulating temperature: Devices for targeted temperature management (TTM) in brain injury. *Intensive Care Medicine*, 48(10), 1409-1412.
13. Fitzgerald, S.; Atkins, H.; Leknys, R.; and Kelso, R. (2018). A thermal test system for helmet cooling studies. *Proceedings of the* 12th *Conference of the International Sports Engineering Association*, Brisbane Queensland Australia.
14. Yacoob, S.M.; and Hassan, N.S. (2012). FDTD analysis of a noninvasive hyperthermia system for brain tumors. *Biomedical Engineering Online*, 11(1), 47.
15. Haeussinger, F.B.; Heinzel, S.; Hahn, T.; Schecklmann, M.; Ehlis, A.-C.; and Fallgatter, A.J. (2011). Simulation of near-infrared light absorption considering individual head and prefrontal cortex anatomy: Implications for optical neuroimaging. *PLoS ONE*, 6(10), e26377.
16. Karaszewski, B. et al. (2008). Early brain temperature elevation and anaerobic metabolism in human acute ischaemic stroke. *Brain*, 132(4), 955-964.
17. Marshall, I.; Karaszewski, B.; Wardlaw, J.M.; Cvoro, V.; Wartolowska, K.; Armitage, P.A.; Carpenter, T.; Bastin, M.E.; Farrall, A.; and Haga, K. (2006). Measurement of regional brain temperature using proton spectroscopic imaging: Validation and application to acute ischemic stroke. *Magnetic Resonance Imaging*, 24(6), 699-706.

18. Karaszewski, B.; Wardlaw, J.M.; Marshall, I.; Cvoro, V.; Wartolowska, K.; Haga, K.; Armitage, P.A.; Bastin, M.E.; and Dennis, M.S. (2006). Measurement of brain temperature with magnetic resonance spectroscopy in acute ischemic stroke. *Annals of Neurology*, 60(4), 438-446.
19. Sahu, Y.K. (2014). *Study on the effective thermal conductivity of fiber reinforced epoxy composites*. MSc dissertation, Department of Mechanical Engineering, National Institute of Technology, Rourkela, India.
20. Abbas, A.; Zhao, Y.; Zhou, J.; Wang, X.; and Lin, T. (2013). Improving thermal conductivity of cotton fabrics using composite coatings containing graphene, multiwall carbon nanotube or boron nitride fine particles. *Fibers and Polymers*, 14(10), 1641-1649.
21. ANSYS, Inc. (2021). *Ansys Fluent theory guide* (*Release* 2021 *R*2). eBook.